

Effect of the initial rotational and vibrational state on the stereodynamics of $\text{N}(^4\text{S})+\text{O}_2(\text{X}^3\Sigma_g^-) \rightarrow \text{O}(^3\text{P})+\text{NO}(\text{X}^2\Pi)$ reaction

Hai-Liang Chen, Zhi-Hong Zhang*, Chuan-Lu Yang, Mei-Shan Wang, and Xiao-Guang Ma

School of Physics and Optoelectronics Engineering, Ludong University, Yantai 264025, the People's Republic of China

Received 10 April 2015; Accepted (in revised version) 9 May 2015

Published Online 6 June 2015

Abstract. The stereodynamics of the atom-molecule reaction $\text{N}(^4\text{S})+\text{O}_2(\text{X}^3\Sigma_g^-) \rightarrow \text{O}(^3\text{P})+\text{NO}(\text{X}^2\Pi)$ has been studied using quasi-classical trajectory method with the lowest $2\text{A}'$ potential energy surfaces (PESs) given by Sayós *et al.* [R. Sayós, C. Oliva, M. González, J. Chem. Phys. 117 (2002) 670]. Four generalized polarization-dependent differential cross-sections $[(2\pi/\sigma)(d\sigma_{00}/d\omega_t), (2\pi/\sigma)(d\sigma_{20}/d\omega_t), (2\pi/\sigma)(d\sigma_{22+}/d\omega_t), (2\pi/\sigma)(d\sigma_{21-}/d\omega_t)]$ and distributions $P(\theta_r), P(\phi_r)$ were calculated. The effects of the different initial rotational and vibrational states were analyzed. It found that the degree of the forward scattering and the product polarizations show obviously change along with the initial vibration number, which leads to the increase of alignment and decrease orientation of product rotational angular momentum j' . Although the influence of the initial rotational excitation effect on the aligned and oriented distribution of product is not stronger than that of the initial vibration excitation effect, the initial rotational excitation makes the alignment of the product rotational angular momentum small change in a certain range. Moreover, the $P(\theta_r)$ distribution and $P(\phi_r)$ distribution change noticeably by varying the initial vibration number.

PACS: 82.20.Fd, 71.15.Pd

Key words: quasiclassical trajectory, vector correlations, stereodynamics, rotational and vibrational excitation.

1 Introduction

The gas-phase reaction $\text{N}(^4\text{S})+\text{O}_2(\text{X}^3\Sigma_g^-) \rightarrow \text{O}(^3\text{P})+\text{NO}(\text{X}^2\Pi)$ and its reverse reaction play an important role in the Earth's atmospheric chemistry [1-2] and combustion processes

*Corresponding author. *Email address:* apzhz@163.com (Z.-H. Zhang)

[3]. This reaction is a source of infrared chemiluminescence in the thermosphere [4]. In previous works, several *ab initio* studies have been reported about the ground $^2A'$ and the first excited $^4A'$ potential energy surfaces (PESs) involved in this reaction. [5-11]. Based on the PESs, some scalar properties of this reaction were studied by using quasiclassical trajectory (QCT) [12-14], the variational transition state theory [8-10], and quantum dynamics methods [15-16], such as the reaction cross-sections, the temperature dependence of the rate constant and the ro-vibrational distributions of product NO molecule. The angular momentum polarizations of the product and the vector correlations between the reagent and product were also calculated with QCT, quantum scattering and wave packet dynamics methods. [17-24] Defazio *et al.* [16] reported the first quantum mechanical calculations of NO rovibrational distributions for the title reaction on the potential energy surface of Sayós *et al.* [7] Ramachandran *et al.* [13] also studied this reaction, but they used QCT on the other PES of Duff *et al.* [25]. It should be noted that their results are in good accord. Meanwhile, on the basis the two PESs, He *et al.* [14] not only calculated the total reaction cross section and the temperature dependence of microscopic rate constants using QCT method, but also compared their results with the experimental results of Gilbert *et al.* [26]. As for the reaction of the vector properties, just recently, Ma *et al.* [27] reported vector correlations between products and reagents for $N(^4S)+O_2(X^3\Sigma_g^-) \rightarrow O(^3P)+NO(X^2\Pi)$ reactions in the different collision energy for the $^2A'$ PES and the $^4A'$ PES. They found that the product rotational angular momentum is more strongly aligned on the $^4A'$ PES than on the $^2A'$ PES at the same collision energy.

As mentioned above, most previous studies basically deal with the scalar properties, such as reaction cross-sections, microscopic and macroscopic rate constants, and rovibrational distributions of the product NO molecule. In this work, we focus on stereodynamics characters of the $N(^4S)+O_2(X^3\Sigma_g^-) \rightarrow O(^3P)+NO(X^2\Pi)$ reaction on the $^2A'$ PES by Sayós *et al.* [7] and comprehensively analyze the effect of the vibrations and the rotational levels of the reactant molecules on the cross-sections and distributions.

2 Computational theory and details

2.1 QCT calculations

In this work, the standard QCT method [28-30] is used to study the stereodynamics of the title reaction based on Sayós *et al.* PES [7]. Only the details relevant to the present reaction will be given here. The initial vibrational and the rotational states of the O_2 molecule were taken to be $v=0-6$ and $j=0, 4, 8, 12, 16, 20, 24, 28, 32, 36$, respectively. Batches of 100000 trajectories were run for each run with an integration step of chosen to 0.1fs and collision energies 1.80eV. The trajectories start at an initial distance of 10 Å between the N atom and the center-of-mass (CM) of the O_2 molecule.

The total reaction cross section is defined as

$$\sigma_r = \pi b_{max} \frac{N_r}{N_T}. \quad (1)$$

Where N_r is the number of reactive trajectories and N_T is the total number of trajectories.

2.2 Vector correlations

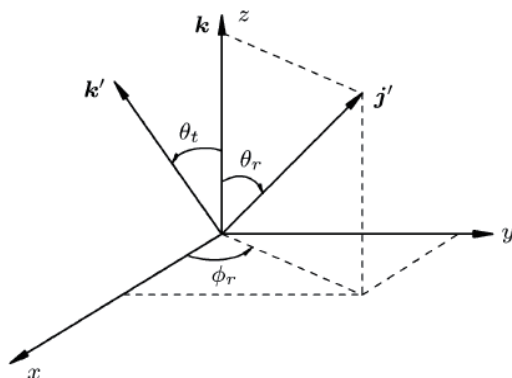


Figure 1: The centre-of-mass coordinate system that describes the correlations k , k' and j' .

The CM frame was used as a reference in the present work, as shown in Fig. 1. The z -axis is parallel to the relative velocity vector k . The $x-z$ plane is the scattering plane that contains the initial and final relative velocity k and k' . θ_t is the scattering angle between the reagent relative and product relative velocity k and k' . θ_r and ϕ_r are the polar and azimuthal angles of the final rotational angular momentum j' , respectively.

The differential cross section (DCS) describes the $k-k'$ distribution or the direction of the product, which is given as follows:

$$\frac{d\sigma_R}{d\omega} = \frac{\sigma_R}{2\pi} \left[\frac{1}{2} + \sum_n a_n P_n(\cos\theta_t) \right]. \quad (2)$$

Where

$$a_n = \frac{2n+1}{2} \langle P_n(\cos\theta_t) \rangle. \quad (3)$$

The distribution function $P(\theta_r)$ describing the $k-j'$ correlation can be expanded in a series of Legendre polynomials as

$$P(\theta_r) = \frac{1}{2} \sum (2k+1) a_0^{(k)}(\cos\theta_r). \quad (4)$$

With

$$a_0^{(k)} = \int_0^\pi P(\theta_r) P_k(\cos\theta_r) \sin\theta_r d\theta_r = \langle P_k(\cos\theta_r) \rangle. \quad (5)$$

The dihedral angle distribution function $P(\phi_r)$ describing $k-k'-j'$ correlation can be expanded in Fourier series as

$$P(\phi_r) = \frac{1}{2\pi} \left(1 + \sum_{\text{even}, n \geq 2} a_n \cos n\phi_r \right) + \sum_{\text{odd}, n \geq 1} b_n \sin n\phi_r. \quad (6)$$

Where

$$a_n = 2\langle \cos n\phi_r \rangle \quad (7)$$

$$b_n = 2\langle \sin n\phi_r \rangle. \quad (8)$$

The vector correlation between the reagent and product can be expressed as

$$P(\omega_1, \omega_r) = \sum_{kq} \frac{2k+1}{4\pi} P_{kq}(\omega_t) C_{kq}(\theta_r, \phi_r)^*. \quad (9)$$

Where $C_{kq}(\theta_r, \phi_r)^* = \sqrt{4\pi/(2k+1)} Y_{kq}(\theta_r, \phi_r)$ is the modified spherical harmonics. And $P_{kq}(\omega_t)$ denotes a generalized polarization-dependent differential cross section (PDDCS), which is defined as

$$P_{kq}(\omega_t) = \frac{1}{\sigma} \frac{d\sigma_{kq}}{d\omega_t} = \int P(\omega_t, \omega_r) C_{kq}(\theta_r, \phi_r) d\omega_r. \quad (10)$$

And $\frac{1}{\sigma} \frac{d\sigma_{kq}}{d\omega_t}$ yields

$$\frac{1}{\sigma} \frac{d\sigma_{kq}}{d\omega_t} = 0, \quad k \text{ is odd.} \quad (11)$$

$$\frac{1}{\sigma} \frac{d\sigma_{kq+}}{d\omega_t} = \frac{1}{\sigma} \frac{d\sigma_{kq}}{d\omega_t} + \frac{1}{\sigma} \frac{d\sigma_{k-q}}{d\omega_t} = 0. \quad (12)$$

k is even and q is odd or k is odd and q is even.

$$\frac{1}{\sigma} \frac{d\sigma_{kq-}}{d\omega_t} = \frac{1}{\sigma} \frac{d\sigma_{kq}}{d\omega_t} - \frac{1}{\sigma} \frac{d\sigma_{k-q}}{d\omega_t} = 0. \quad (13)$$

k is odd and q is even or k is odd and q is odd.

PDDCS can then be written as

$$\frac{1}{\sigma} \frac{d\sigma_{kq\pm}}{d\omega_t} = \sum_{k_1} \frac{[k]}{4\pi} S_{kq\pm}^{k_1} C_{k_1q\pm}(\theta_t, 0). \quad (14)$$

Where $S_{kq\pm}^{k_1}$ is evaluated from the expected expression

$$S_{kq\pm}^{k_1} = \langle C_{k_1q}(\theta_t, 0) C_{kq}(\theta_r, 0) \rangle [(-1)^q e^{iq\phi_r} \pm e^{-iq\phi_r}]. \quad (15)$$

The angular brackets represent an average over all angles. The DCS is given by

$$\frac{1}{\sigma} \frac{d\sigma_{00}}{d\omega_t} = P(\omega_t) = \frac{1}{4\pi} \sum_{k_1} [k_1] h_0^{k_1}(k_1, 0) P_{k_1}(\cos\theta_t). \quad (16)$$

$h_0^{k_1}(k_1, 0)$ are evaluated by the expectation values of the Legendre moments of the differential cross-section as follows:

$$S_{00}^k = h_0^k(k, 0) = \langle P_k(\cos\theta_t) \rangle. \quad (17)$$

For $q=0$, PDDCS is given as

$$\frac{1}{\sigma} \frac{d\sigma_{00}}{d\omega_t} = \frac{1}{4\pi} [k_1] S_{k0}^{k_1} P_{k_1}(\cos\theta_t). \quad (18)$$

Where σ is the integral cross section and $(1/\sigma)(d\sigma_{kq}/d\omega_t)$ are the generalized polarization dependent differential cross section (PDDCSs) [31-32]. $(2\pi/\sigma)(d\sigma_{00}/d\omega_t)$, $(2\pi/\sigma)(d\sigma_{20}/d\omega_t)$, $(2\pi/\sigma)(d\sigma_{22+}/d\omega_t)$, and $(2\pi/\sigma)(d\sigma_{21-}/d\omega_t)$ were calculated in this work.

3 Results and discussion

3.1 Generalized PDDCSs

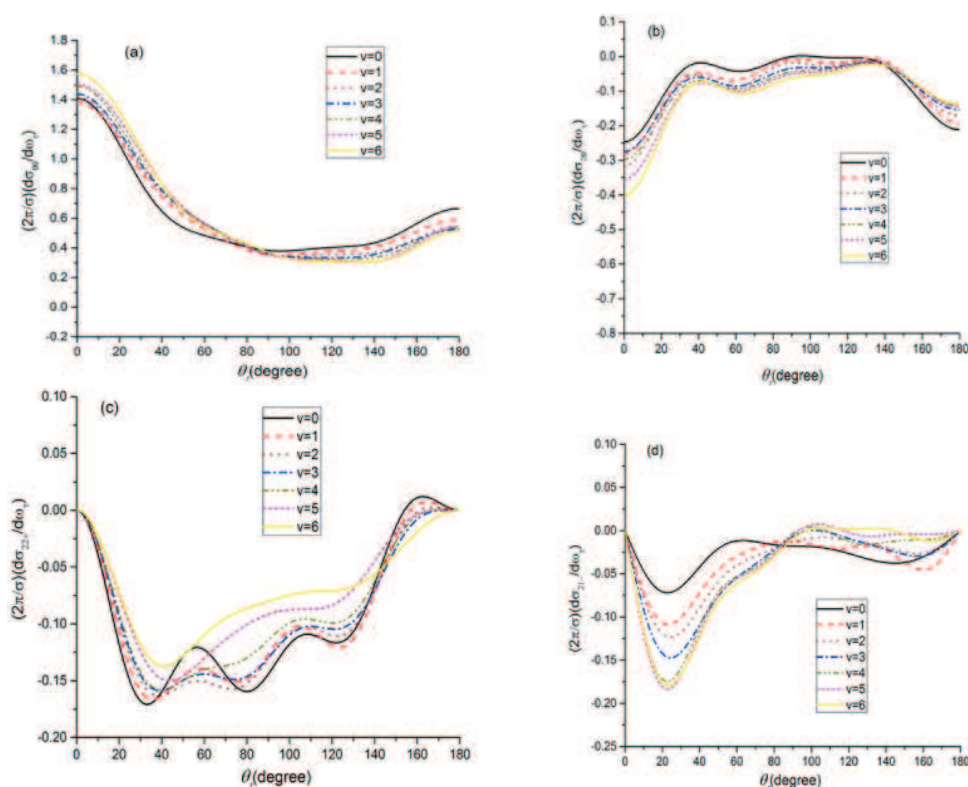


Figure 2: Polarization-dependent differential cross section in the different initial vibrational excitation states. (a) $(2\pi/\sigma)(d\sigma_{00}/d\omega_t)$; (b) $(2\pi/\sigma)(d\sigma_{20}/d\omega_t)$; (c) $(2\pi/\sigma)(d\sigma_{22+}/d\omega_t)$; and (d) $(2\pi/\sigma)(d\sigma_{21-}/d\omega_t)$.

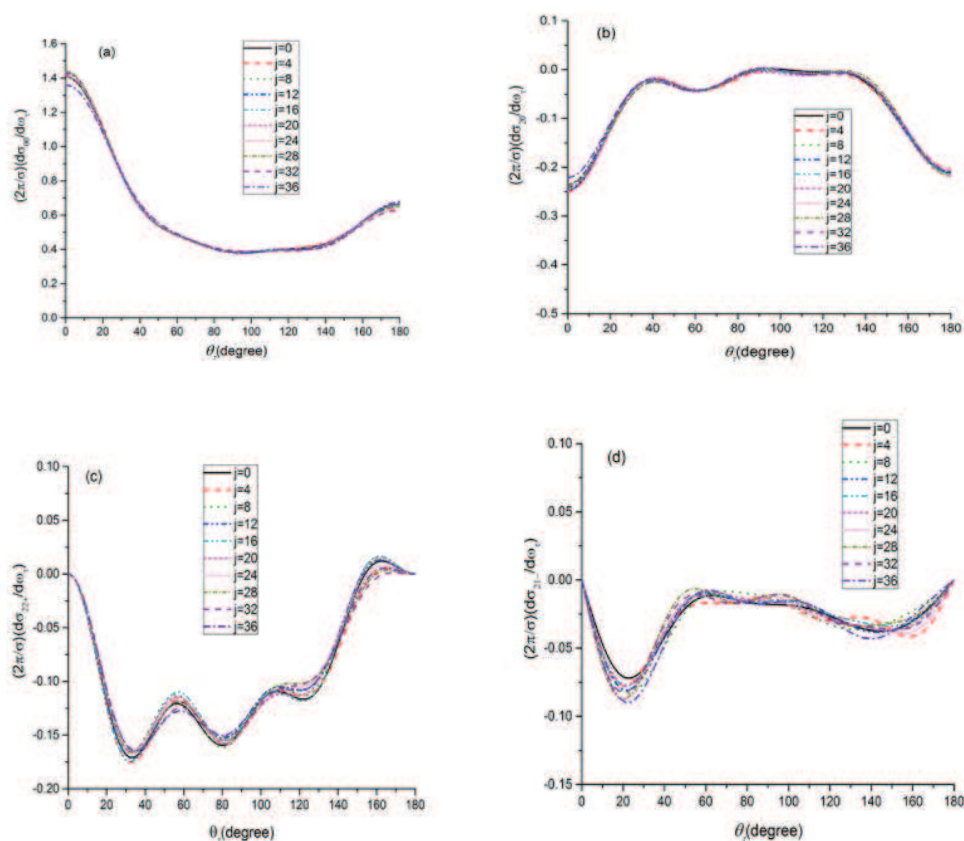


Figure 3: The same as Fig. 2 but in the different initial rotational excitation states.

The PDDCSs describes the $k-k'-j'$ correlation and the scattering direction of the product molecule NO. Fig. 2 and 3 show the PDDCSs of the title reaction with the vibrational and the rotational states ($v=0-6, j=0$), ($j=0-36, v=0$) and $E_c=1.80\text{eV}$, respectively. The PDDCSs $(2\pi/\sigma)(d\sigma_{00}/d\omega_t)$ is simply describing the $k-k'$ correlation, i.e., the differential cross section (DCS). The scattering direction of the product NO is related to the vibrational and the rotational quantum number. As is shown in Fig. 2a and 3a, the product angular mainly distributed in forward directions and accompanied by the small backward scattering. Besides, the tendency of the forward scattering is gradually stronger and the backward scattering reduces remarkably with increasing v . However, the effect of the rotational excitation is extremely weak for the degree of scattering. The PDDCS $(2\pi/\sigma)(d\sigma_{20}/d\omega_t)$ is related to the expectation value of the second Legendre moment $\langle P_2(\cos(\theta_r)) \rangle$, which contains the alignment information of j' with respect to k . As is shown in Fig. 2b and 3b, an opposite distribution trend to that in the $(2\pi/\sigma)(d\sigma_{00}/d\omega_t)$ and obviously depends on the scattering angle θ_t . It is easy to know from Fig. 2 (b) the $(2\pi/\sigma)(d\sigma_{20}/d\omega_t)$ values of the title reaction are negative for forward and backward scattering, but the values are close to zero for the sideways scattering. The negative

values of $(2\pi/\sigma)(d\sigma_{20}/d\omega_t)$ close to the 180° decrease with increasing v , which indicates that the trend of j (perpendicular to k is more prominent for the lower vibration of quantum number. The distributions of $(2\pi/\sigma)(d\sigma_{22+}/d\omega_t)$ and $(2\pi/\sigma)(d\sigma_{21-}/d\omega_t)$ with $q \neq 0$, which are close to zero at the extremities of forward and backward scattering. It can be seen from Fig. 2 (c) and 3 (c) that the $(2\pi/\sigma)(d\sigma_{22+}/d\omega_t)$ values of the $\text{N}(^4\text{S})+\text{O}_2(\text{X}^3\Sigma_g^-) \rightarrow \text{O}(^3\text{P})+\text{NO}(\text{X}^2\Pi)$ reaction are slightly positive for the scattering angles 150° . These results suggest that the alignments of the NO product are along both x -axis and y -axis, but the product mainly along the y -axis. Furthermore, the products NO display a strong polarization at about 30° and 150° . The PDDCS $(2\pi/\sigma)(d\sigma_{21-}/d\omega_t)$ is related to $\langle \sin^2\theta_r \cos^2\phi_r \rangle$ (2d and 3d). The product NO exhibits a strong polarization. Especially, when the angle θ_t is at about 25° the product NO of polarization is gradually stronger along with the increase of v . These results suggest that the product angular distribution is anisotropic for the reaction. The anisotropy of the reaction is gradually weaker with increasing v .

3.2 $k-j'$ vector correlations

To gain insight into the stereodynamics of the reaction, we investigate the $k-j'$ vector correlations and $k-k'-j'$ vector correlation. The $P(\theta_r)$ distributions of the product NO describe the $k-j'$ correlations at the vibrational and the rotational different quantum number, which are shown in Fig. 4 and, respectively.

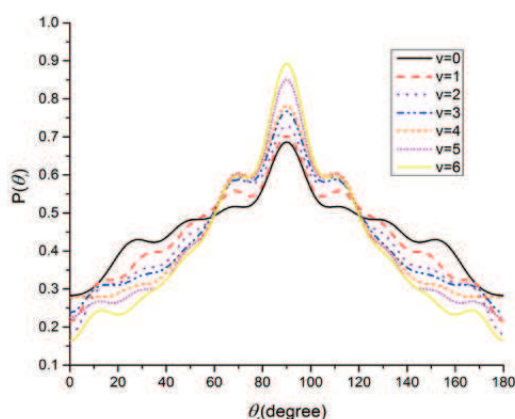


Figure 4: $P(\theta_r)$ distribution that describes the $k-j'$ correlation in the different initial vibrational excitation states.

In this case, the $P(\theta_r)$ distributions have a maximum for θ_r close to 90° and symmetric with respect to 90° . The calculated results indicate that the product rotational angular momentum vector (j') is strongly aligned along the direction at right angle to the relative velocity direction. As shown in Fig. 4, the peak of the $P(\theta_r)$ distribution gradually stronger with increases in v from 0 to 6. The value of the $P(\theta_r)$ distribution is maximum

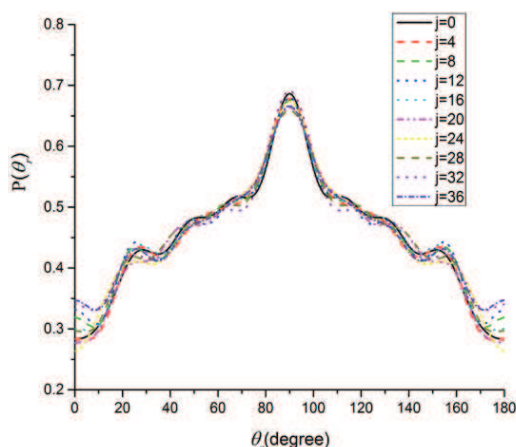


Figure 5: Similar to Fig. 4 but in the different initial rotational excitation states.

for $v=6$. It is believed that the reagent vibrational excitation enhances the anisotropic distribution of the product rotational angular momentum alignment.

Table 1: Values of the product alignment parameter $\langle P_2(j' \cdot k) \rangle$.

$\langle P_2(j' \cdot k) \rangle$ reaction states	$v=0,$ $j=0$	$v=1,$ $j=0$	$v=2,$ $j=0$	$v=3,$ $j=0$	$v=4,$ $j=0$	$v=5,$ $j=0$	$v=6,$ $j=0$
N + O ₂	-0.375	-0.386	-0.396	-0.403	-0.407	-0.414	-0.423

For the $\text{N}(^4\text{S})+\text{O}_2(\text{X}^3\Sigma_g^-) \rightarrow \text{O}(^3\text{P})+\text{NO}(\text{X}^2\Pi)$ reaction, the value of the product alignment parameter decreases from -0.38 ($v=0, j=0$) to -0.42 ($v=6, j=0$). This is confirmed by the values of the product alignment parameter $\langle P_2(j' \cdot k) \rangle$. The results are presented in Table 1, where the value of the product alignment parameter is smaller and smaller along with the increase of initial vibrational quantum number. Therefore, the stronger alignment of the rotational angular momentum takes place in the high initial vibrational excitation state. When the reagent becomes rotationally excited, the $P(\theta_r)$ distributions decrease to a certain extent (Fig. 5). This phenomenon directly reflects that the alignment of angular momentum does not show obvious anisotropy for initial rotational excitation states.

3.3 $k-k'-j'$ vector correlations

The behavior of the $P(\phi_r)$ distribution of the $\text{N}(^4\text{S})+\text{O}_2(\text{X}^3\Sigma_g^-) \rightarrow \text{O}(^3\text{P})+\text{NO}(\text{X}^2\Pi)$ reaction is shown in Fig. 6 and 7, which describe $k-k'-j'$ correlation in the different initial vibrational and rotational excitation state ($v=0-6, j=0$), ($j=0-36, v=0$), respectively.

It can be obviously seen from Fig. 6 that the peak of $P(\phi_r)$ distribution at $\phi_r=270^\circ$ is distinctly stronger than that at $\phi_r=90^\circ$. This phenomenon indicates that the rotational angular momentum vector of the product j' tends to be oriented along the negative direction

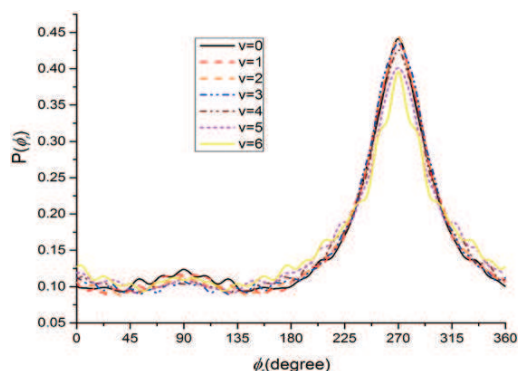


Figure 6: $P(\phi_r)$ distribution for j' with respect to the $k-k'$ plane in the different initial vibrational excitation states.

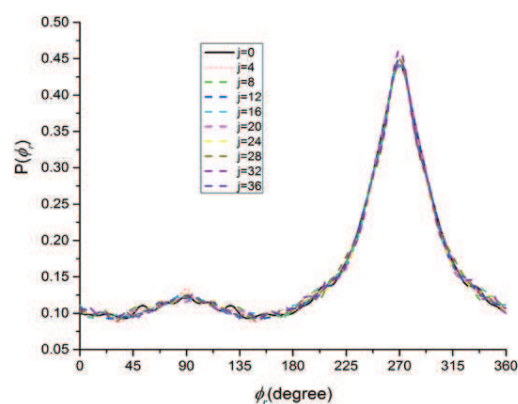


Figure 7: Similar to Fig. 6 but in the different initial rotational excitation states.

of the y -axis. In addition, the value of the $P(\phi_r)$ distribution at $\phi_r=270^\circ$ decreases along with the enhancement of the vibrational excitation, which mean the reaction is dominated by the in-plane reaction mechanism. For the initial rotational excitation, the peak of $\phi_r=270^\circ$ is still the main distribution (Fig. 7). It means that the rotation of NO tends to be oriented along the negative direction of the y -axis. In short, the product polarization of reaction is considerably sensitive to the vibrational excitation of the reagent.

4 Conclusions

The QCT calculations have been carried out to study the initial rotational and vibrational effect of the reactant molecule on the stereodynamic properties of the $\text{N}(^4\text{S})+\text{O}_2(^3\Sigma_g^-) \rightarrow \text{O}(^3\text{P})+\text{NO}(^2\Pi)$ reaction. Four PDDCSs and the distributions of $P(\theta_r)$, and $P(\phi_r)$ have been calculated. The $(2\pi/\sigma)(d\sigma_{00}/d\omega_t)$ indicates that the angular distributions of NO products are mainly forward asymmetry scatterings. Moreover, the $P(\theta_r)$ indicates that the product rotational angular momentum j' is strongly aligned along the direction at right angle to the relative velocity direction(k) at the initial rotational and vibrational

states, however, the effect of initial rotational on the $P(\theta_r)$ distribution is almost negligible. The distributions of $P(\phi_r)$ for the title reaction indicate that the product rotational angular momentum j' is not only aligned, but also oriented along the negative direction of the y -axis. In one word, the initial rotational and vibrational excitations of the reagent have a strong influence on the product rotational polarization. The reactive probabilities are strongly dependent on the initial vibration quantum state.

Acknowledgments. This work was supported by the National Science Foundation of China (NSFC) under Grant Nos. NSFC-11174117 and NSFC-11374132. Many thanks should be given to Prof. Keli Han for providing QCT code for stereodynamics.

References

- [1] M.W. Chase Jr., C.A. Davies, J.R. Downey Jr., D.J. Frurip, R.A. McDonald, A.N. Syverud, J. Phys. Chem. Ref. Data 14 (1985) 1.
- [2] D.L. Baulch, C.J. Cobos, R.A. Cox, G. Hayman, T. Just, J.A. Kerr, T. Murrells, M.J. Pilling, J. Troe, R.W. Walker, J. Warnatz, J. Phys. Chem. Ref. Data 23 (1994) 873.
- [3] T.C. Corcoran, E.J. Beiting, M.O. Mitchell, J. Mol. Spectrosc. 154 (1992) 119.
- [4] P. Warneck, Chemistry of the Natural Atmosphere, Academic, San Diego, 1998 (Chapter 3).
- [5] M. Gilibert, A. Aguilar, M. González, R. Sayós, Chem. Phys. 172(1993) 99.
- [6] M. Gilibert, X. Giménez, M. González, R. Sayós, A. Aguilar, Chem. Phys. 191 (1995) 1.
- [7] R. Sayós, C. Oliva, M. González, J. Chem. Phys. 115 (2001) 1287.
- [8] R. Sayós, C. Oliva, M. González, J. Chem. Phys. 117 (2002) 670.
- [9] R. Sayós, J. Hijazo, M. Gilibert, M. González, Chem. Phys. Lett. 284 (1998) 101.
- [10] G.S. Valli, R. Orrú, E. Clementi, A. Laganá, S. Crocchianti, J. Chem. Phys. 102 (1995) 2825.
- [11] M. González, C. Oliva, R. Sayós, J. Chem. Phys. 117 (2002) 680.
- [12] P.J.B.S. Caridade, A.J.C. Varandas, J. Phys. Chem. A 108 (2004) 3556.
- [13] B. Ramachandran, N. Balakrishnan, A. Dalgarno, Chem. Phys. Lett. 332 (2000) 562.
- [14] J.F. He, S.X. Liu, X.S. Liu, P.Z. Ding, Chem. Phys. 315 (2005) 87.
- [15] P. Defazio, C. Petrongolo, S.K. Gray, C. Oliva, J. Chem. Phys. 115 (2001) 3208.
- [16] P. Defazio, C. Petrongolo, C. Oliva, M. González, R. Sayós, J. Chem. Phys. 117 (2002) 3647.
- [17] K.L. Han, G.Z. He, N.Q. Lou, J. Chem. Phys. 105 (1996) 8699.
- [18] M.L. Wang, K.L. Han, G.Z. He, J. Chem. Phys. 109 (1998) 5446.
- [19] M.D. Chen, M.L. Wang, K.L. Han, S.L. Ding, Chem. Phys. Lett. 301 (1999) 303.
- [20] F.J. Aoiz, L. Bañares, J.F. Castillo, B. Martínez-Haya, Marcelo P. deMiranda, J. Chem. Phys. 114 (2001) 8328.
- [21] M.D. Chen, K.L. Han, N.Q. Lou, Chem. Phys. Lett. 357 (2002) 483.
- [22] M.D. Chen, K.L. Han, N.Q. Lou, Chem. Phys. 283 (2002) 463.
- [23] M.D. Chen, K.L. Han, N.Q. Lou, J. Chem. Phys. 118 (2003) 4463.
- [24] I. Miquel, J. Hernando, R. Sayós, M. González, J. Chem. Phys. 119(2003) 10040.
- [25] J.W. Duff, F. Bien, D.E. Paulsen, Geophys. Res. Lett. 21 (1994) 2043.
- [26] M. Gilibert, A. Aguilar, M. González, R. Sayós, Chem. Phys. 178 (1993) 287.
- [27] J.J. Ma, M.D. Chen, S.L. Cong, K.L. Han, Chem. Phys. 327 (2006) 531.
- [28] K.L. Han, G.Z. He, N.Q. Lou, J. Chem. Phys. 105 (1996) 8699.
- [29] X. Zhang, K.L. Han, Int. J. Quantum Chem. 106 (2006) 1815.
- [30] K.L. Han, L. Zhang, D.L. Xu, G.Z. He, N.Q. Lou, J. Phys. Chem. A 105 (2001) 2956.

- [31] N.E. Shafer-Ray, A.J. Orr-Ewing, R.N. Zare, J. Phys. Chem. A 99 (1995) 7591.
- [32] F.J. Aoiz, M. Brouard, P.A. Enriquez, J. Chem. Phys. 105 (1996) 4964.